Laser-assisted guiding of electric discharges around objects

Laser-Assisted Guiding of Electric Discharges around Objects

Authors: M. Clerici[1,2]*, Y. Hu[1,3], P. Lassonde[1], C. Milián[4], A. Couairon[4], D. Christodoulides[5], Z. Chen[3,6], L. Razzari[1], F.Vidal[1], F. Légaré[1], D.Faccio[2], R. Morandotti[1,7]*

Affiliations:

[1]INRS-EMT, 1650 Blvd. Lionel-Boulet, Varennes, Québec J3X 1S2, Canada.

[2]School of Engineering and Physical Sciences, SUPA, Heriot-Watt University, Edinburgh EH14 4AS, UK.

[3]The MOE Key Laboratory of Weak Light Nonlinear Photonics, School of Physics and TEDA Applied Physics School, Nankai University, Tianjin 300457, China.

[4]Centre de Physique Théorique CNRS, École Polytechnique, F-91128 Palaiseau, France.

[5]College of Optics - CREOL, University of Central Florida, Orlando, Florida 32816, USA.

[6]Department of Physics and Astronomy, San Francisco State University, San Francisco, California 94132, USA.

[7]Institute of Fundamental and Frontier Sciences, University of Electronic Science and Technology of China, Chengdu 610054, PR China.

*Correspondence to: clerici@hw.ac.uk, morandotti@emt.inrs.ca

Abstract: Electric breakdown in air occurs for electric fields exceeding 34 kV/cm and results in a large current surge that propagates along unpredictable trajectories. Guiding such currents across specific paths in a controllable manner could allow protection against lightning strikes and high voltage capacitor discharges. Such capabilities can be employed for delivering charge to specific targets, electronic jamming or for applications associated with electric welding and

machining. Here we show that judiciously shaped laser radiation can be effectively utilized to manipulate the discharge along a complex path and to produce electric discharges that unfold along a predefined trajectory. Remarkably, such laser induced arcing can even circumvent an object that completely occludes the line of sight.

One Sentence Summary: We demonstrate that laser beam shaping can be employed to precisely control an electric discharge trail, avoiding or bypassing obstacles in the line of sight.

Main Text:

Introduction

Since the dawn of civilization, electric discharge phenomena such as lightning have played a key role in the scientific understanding of electricity itself. Today, these same processes are an integral part of modern technologies and find applications in numerous settings. In gases, they typically occur when the applied voltage between two electrodes establishes a field that exceeds breakdown, which in air is approximately 34 kV/cm under standard conditions for temperature and pressure. In manufacturing, arc discharges are routinely employed for machining *(1)* and micromachining *(2)*, and for assisting the milling process *(3)*. They are also used for fuel ignition in combustion engines *(4–6),* as a means to control the hydrodynamics of high speed gasses *(5,6)* and could ultimately be utilized in monitoring and controlling pollution *(7,8)*. Yet, in spite of such advances, developing methods to effectively control and shape the path of an electrical spark along a predetermined trajectory still remains a significant challenge.

Clearly, it will be of fundamental importance to devise schemes through which arcing can be fully controlled. In this work, we show that properly shaped laser beams can provide a means to this end by virtue of the ionization they induce in air, see Fig. 1 [for earlier works on laser-

assisted electric discharges see e.g. *(9–13)*, and for the latest investigations see e.g. *(14,15)*]. The recent introduction of self-bending Airy beams in optics (Fig. 1C) has opened up new opportunities in terms of propagating spatially accelerating wavefronts along complex curved trajectories *(16)*, and here we demonstrate that it can also provide a new degree of freedom in controlling electric discharges. By manipulating the specific shape of a laser beam, it is indeed possible to precisely control the trail of a spark. Along these lines, parabola-like and S-shaped electrical discharges can be achieved (see Figs. 1 and 2), thus transporting the electrical charge around objects that would have otherwise completely blocked the discharge itself. Another important attribute of an Airy beam is the ability to spontaneously reform its main intensity features after encountering an obstacle. This property, referred to as self-healing, is shared also by another important class of sub-diffractive beams, the so-called Bessel beams, Fig. 1B, *(17)*. Remarkably, we show that the self-healing properties of Airy and Bessel laser wavefronts can be readily transferred to the electrical discharge, which also self-heals and resumes its original trajectory even after a direct hit on an obstacle. In this regard, not only the unpredictability that usually accompanies this phenomenon is removed, but the discharge can also be manipulated in a way such that the resulting arc can bypass an object placed in the line of sight between the two electrodes.

Results

As a reference, we first consider the case where a standard Gaussian beam guides the discharge (as illustrated in Fig. 1A). We focused the Gaussian beam delivered by an amplified Ti:Sapphire system with a lens (focal length f=100 cm) between two wire electrodes. The input energy is 15 mJ, the beam full-width at half maximum is 10 mm and the pulse duration is 50 fs. After an optical filament is formed *(18)*, the laser pulse ionizes the air between the electrodes, as can be

seen from the resulting fluorescence shown in Fig. 2A, and deposits energy that induces an expanding heat wave. In turn, the heated air column locally reduces the gas density, thus lowering the breakdown voltage over a path defined by the laser induced ionization (*19,20*), since the electron avalanche process depends on E/N, where E and N are the local electric field strength and air density, respectively (*21*). When a relatively high voltage is applied (nearly 15 kV over a 5 cm gap - a field far lower than that for the air breakdown at 1 atm), a discharge occurs between the electrodes and, more importantly, it follows the path of the least resistance, i.e. along the trajectory determined by the laser beam (see Fig. 2B). Note that in this case the arc trail is heavily distorted and effectively unpredictable. In Figs. 2C and 2D we present the case of a discharge triggered and guided by a Bessel beam with a 4.6 degree cone-angle as obtained by means of a fused-silica axicon with a 10 degree base-angle for electrodes distance and an applied voltage equal to the previous case. The central high intensity peak of the sub-diffractive Bessel beam has a diameter of ~7 μm and is thus much smaller than the diameter of the Gaussian optical filament (~50 μm). As a result, the plasma excitation is more localized in the transverse direction (Fig. 2C) and the electric discharge (Fig. 2D) is thus guided along a much better defined path, with no evidence of random jumps as seen in Fig. 2B. We then repeat this same experiment (i.e., for the same voltage and electrodes distance) with a self-bending beam that is generated by employing an aberrated cylindrical lens system (*22*). This beam propagates along a curved parabolic trajectory with a sub-diffractive intensity peak of nearly 20 μm diameter. As shown in Fig. 2E, the induced plasma follows the curved excitation by the laser pulse (*23*) [this is also the case for plasmonic Airy and Bessel beams (*24,25*)] and, most importantly, we observe that the electric discharge also occurs along the same curved path (see Fig. 2F). As presented in the figure, the self-bending beam is capable of creating a plasma channel that circumvents an

obstacle (the edge of an opaque glass) that would have otherwise blocked the direct line of sight between the two electrodes. In other words, the discharge follows the plasma trajectory and thus travels around the obstacle without damaging (via corona discharge) the object itself. Finally, more complex arc shapes can be easily realized. For example, by using a binary phase mask that transforms the input laser pulse into two concatenated Airy beams, an S-shaped plasma channel is produced as shown in Fig. 2G. Clearly, also in this case, the electric discharge is guided along the pre-assigned path (Fig. 2H).

We further investigated the electric breakdown for the three cases as shown in Fig. 1. We observed a significant reduction of the breakdown field (compared to the standard unguided configuration) that is 3.5 and 10 times lower for the cases of the self-bending and of the Bessel beam, respectively (see Supplementary Materials). Therefore we estimate that a guided discharge may be supported along any arbitrary trajectory [see e.g. (*26–30*)] that has at least a ratio of 3.5 between the arc-length and the inter-electrode distance.

We then perform experiments where an obstacle is placed directly in the beam path so that it completely blocks the main intensity peak of the laser pulse. For the case of a standard Gaussian beam, this results in a complete quenching of the beam and no light is transmitted. As shown in Fig. 3A, the conductive channel is also obstructed and no discharge occurs when the potential is applied between the two electrodes (Fig. 3B). The situation is completely different in the case of non-diffracting laser beams. Indeed, for such waveforms, it has been demonstrated that even if the main intensity peak is blocked while the remaining part of the beam is allowed to pass, self-healing takes place (*31–33*) and the intense part of the beam reconstructs itself after encountering an obstacle. This can be clearly seen in Figs. 3C and 3E, where the plasma fluorescence generated by a Bessel and an Airy beam, respectively, re-appears after few millimeters, beyond

an opaque screen that is placed in the beam path. As a consequence, we observe that the electric discharge channel can also self-heal so that it may propagate between the two electrodes (see Figs. 3D and 3F). We note that in the region immediately after the obstacle, where the laser beam has not healed yet and is thus not able to substantially ionize the medium, the electric path is actually random from one laser shot to the next (see inset in Fig. 3D). However, it is the presence of the healed plasma channel after the obstacle that ensures that the discharge actually occurs and follows a well-defined path along the optical beam trajectory. This result also holds in the case of an isolated conductive obstacle (see Supplementary Materials).

A deeper understanding of the complex physics associated with the discharge self-healing process can be obtained by considering numerical models for describing the optical spatio-temporal dynamics as well as the onset of the electric arc. The numerical solution to this problem is obtained in a three-step procedure (see Supplementary Materials for more details), consisting of: 1) the simulation of the nonlinear pulse propagation that "deposits" energy in the gas via field ionization (neglecting collisional processes) (*19,34*), 2) the simulation of the gas hydrodynamics under non-equilibrium conditions resulting from the heating associated to the plasma recombination (*35,36*) and, finally 3) the simulation of the electric discharge that takes place along the lower gas density channel determined by the gas hydrodynamics (*37*). We note that the electric discharge process does not interfere with the creation of the plasma induced by the focused laser since it occurs after several nanoseconds from the laser pulse passage. As an example, we focused our attention on the case of an object placed in the path of a diffraction-free Bessel beam.

In this regard, we simulated the pulse propagation using parameters that are compatible to those encountered in our experiment (*18*). The gas temperature increase (T) induced by the laser pulses

on the gas medium is estimated from the observed breakup voltage by means of the Paschen law, as detailed in the Supplementary Materials. In the case of a Bessel beam and for the parameters used in our experiment, beam dynamics leads to a local temperature rise of nearly 50,000 K. Using this temperature increase as an input condition we simulated the gas hydrodynamics and we found that a large density depression is established on axis after 6.5 ns and the gas density decreases to 7% of the normal gas density. Figure 4A shows the air density map obtained via this hydrodynamic simulation considering a 2-mm width stopper in the beam path. We then simulated the discharge propagation using a stochastic model similar to that employed by Niemeyer et al. (*37*). To do so, we assumed a growth probability $P_i \cong \left(E_i/N_i\right)^5 \Big/ \sum_j \left(E_j/N_j\right)^5$ where the index i denotes the possible leader growth directions at a given time step. Here the electric field E_i is obtained by solving the two-dimensional Laplace equation for the electric potential while the air density N_i is determined from the hydrodynamic simulation (Fig. 4A). In this model, leaders start simultaneously from both electrodes, when E_i/N_i is greater than some threshold values, and meet in between to bridge the air gap. The simulation (Fig. 4B) shows that the discharge follows closely the rectilinear air-depleted path left by the laser while it is wandering with a few millimiters deviation from the straight trajectory in the ~1-cm region past the dielectric stopper - where the Bessel beam is partly quenched. These predictions are in good agreement with our experimental results.

We note that the discharge self-healing process is restrained by the intrinsic limitations of the optical self-healing, and also by the requirement that the available potential difference at the electrodes is sufficient to generate a field higher than that of the breakdown across the broken plasma channel. For example, for the case of the Bessel beam investigated here, our 35 kV DC source will discharge over a maximum distance of the order of 1 cm, corresponding to an

obstacle width of ~1.6 mm (that determines the distance over which the Bessel channel self-heals). This prediction is compatible with our experimental observations. If we upscale the DC potential e.g. to 1 MV and also the laser power/optical elements aperture in order to extend the length of the laser ionized channel, we may speculate that the maximum allowed obstacle width could scale to ~5 cm.

Discussion

The proposed technology paves the way to the systematic and precise control of a high voltage discharge along predetermined paths and provides a new degree of freedom in controlling electrical discharge-driven phenomena, opening an array of possibilities for both scientific and technological settings. We have shown that Airy and Bessel beams allow the discharge to circumvent obstacles, to propagate along a defined path (avoiding an erratic, lightening-like trajectory), and to self-heal in the presence of an obstacle. Other beam geometries, such as nonparaxial accelerating beams (*26–30*) and plasma waveguide arrays (*38*), may play an essential role in the further development of this new and powerful degree of control. For example, two skewed Bessel beams may be employed to trigger an arc in gas at a remote location, while other configurations (such as abruptly autofocusing beams) can be used to induce arcing with very high spatial accuracy. The development of reconfigurable (telescopic like) systems of refractive or holographic optics that can dynamically control both the beam trajectories and bending angles of optical pulses with intensities sufficient to induce air ionization in the region of interest will be instrumental for the technological impact of the proposed ideas.

Finally, in a two-pulse excitation scheme, the plasma length is enhanced by properly choosing the delay between the pulses - due to the response associated to the molecular alignment (*39*),

and may thus be considered as a further degree of freedom to control laser guided electric discharges.

Materials and Methods

We have modeled the experimental observation of laser guided electric discharge, with or without an obstacle in the beam-path, by considering, without loss of generality, the case of a Bessel beam. A first step consists in computing the nonlinear propagation of the optical pulse generated by our laser source in air, accounting for the space-time effects as detailed in the Supplementary Material. By considering a Gaussian pulse with a full width at half maximum (FWHM) of 50 fs, an energy of 15 mJ, a beam width of 1 cm FWHM, and a 800 nm wavelength, focused by an axicon with a cone angle of 4.6 degrees, we observed that the peak intensity of the pulse reaches nearly 10^{14} W/cm^2, and remains fairly constant over more than 10 cm, thus ionizing the totality of oxygen and nitrogen molecules. We also investigated the dynamics of the laser-induced ions and free carriers subsequent to the laser passage. Following the model proposed by Zhao et al. *(40)*, we found that fractions of a nanosecond after the pulse transits, electron-ion recombination nearly neutralizes the medium. We hence simulated the hydrodynamic expansion of heated air by solving the compressible fluid Euler equations in two-dimensional cylindrical coordinates. The integration of the fluid equations is carried out through the Harten Lax van Leer first order Godunov method with the restoration of the contact wave, HLLC *(35)*. The system of equations is closed by means of the equation of state and the internal energy in the ideal gas forms. The initial condition in the simulation consists of a temperature distribution that follows from the shape of the plasma generated by the laser. More specifically, we considered the first lobe of a Bessel function interrupted by a stopper and self-healed, as can be deduced by observing the fluorescence in Fig. 3C of the main text. For more details on the

model and on the self-healing length, see Supplementary Material. The gas temperature was evaluated considering the Paschen law ($V_B \propto \rho$, where V_B is the breakdown voltage and ρ the gas density) together with the observed experimental decrease of V_B by an order of magnitude with respect to the case of unheated air and for the Bessel beam case. In the Supplementary Materials we provide a detailed discussion on the experimental evaluation of this factor for three beam profiles (Gaussian, Self-bending and Bessel). This leads to a temperature increase of the order of $\Delta T \approx 50{,}000$ K. To model the discharge evolution between the two electrodes, we adopted a stochastic model similar to that of Niemeyer et al. *(37)*. A detailed account of the simulation parameters that provide results in agreement with the experimental observations is given in the Supplementary Material.

Figure1

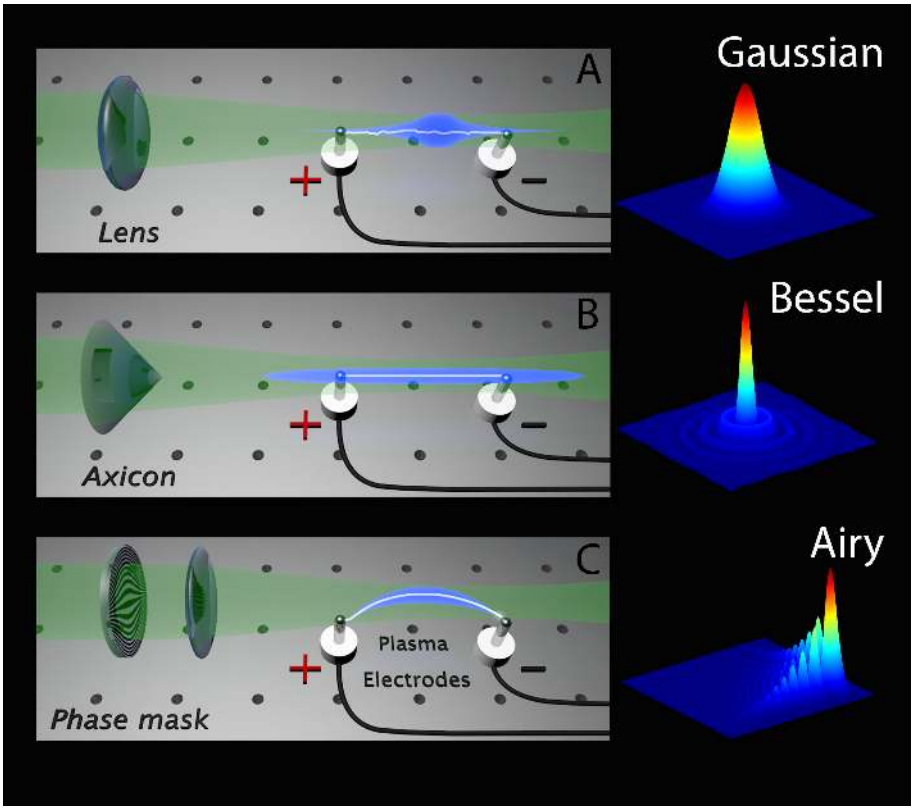

Figure 1. Laser guided discharges. (Left panels) Electric discharges resulting from different beam shaping configurations. These include: (**A**) - a standard Gaussian beam focused by a lens; (**B**) - a Bessel beam formed after an axicon; (**C**) – an Airy beam produced by a binary phase mask. The laser is represented in green, the plasma channel is in blue, and the discharge is depicted in white. The right panels show the intensity distribution corresponding to the different beam shaping configurations.

Figure 2

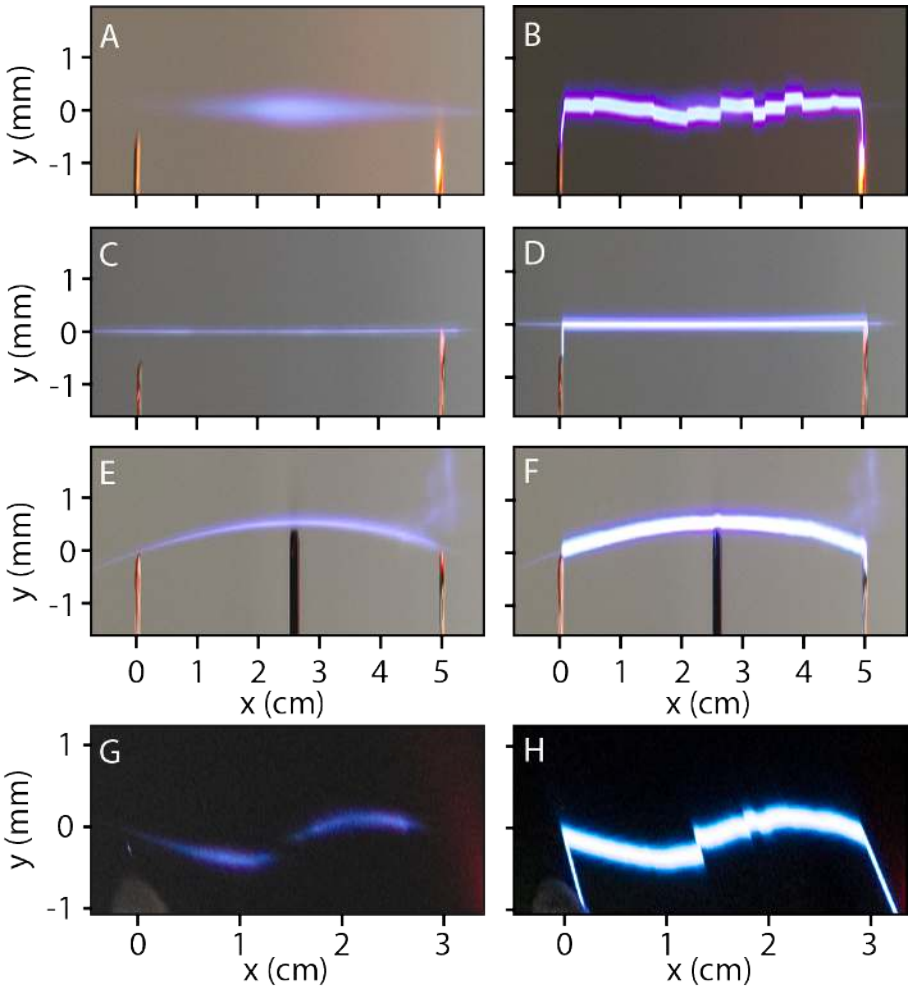

Figure 2. Shaped laser plasmas and electric discharges. Different shapes associated to the discharges that can be achieved through judicious beam shaping. (**A**) is for a Gaussian, (**C**) is for a Bessel, (**E**) is for an Airy and (**G**) is for a S-shaped beam obtained by properly combining two conventional Airy beams. The left panels are the photographs taken when no voltage is applied (showing the laser beam path through ionization-induced fluorescence) and the right panels show the discharge in the presence of a high voltage between the two electrodes.

Figure 3

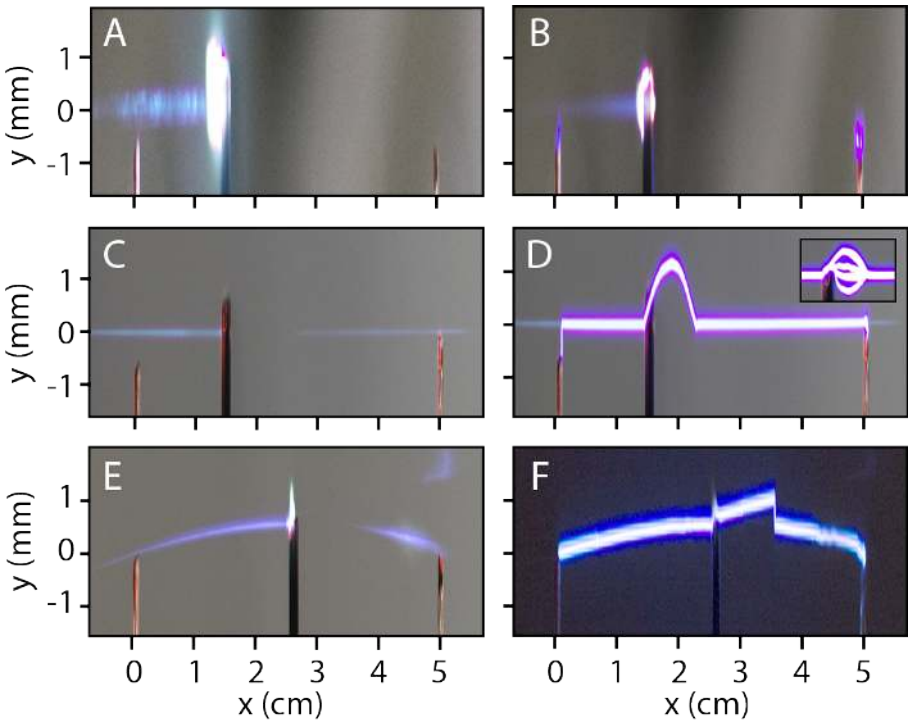

Figure 3. Effect of an obstacle placed in the control beam path. (**A**), (**C**) and (**E**) show how the intense part of the beam (the blue fluorescence in the photographs) is modified upon the insertion of an object in the beam path for a Gaussian, a Bessel, and an Airy beam, respectively. In the Gaussian case, the intensity of the beam is completely quenched after the obstacle and there is no way to guide an electric discharge between the two poles shown in (**B**). On the other hand, for both the cases of a Bessel and of an Airy type propagation the beam restores itself after the obstacle and the electric discharge occurs along an almost unaffected trajectory (**D** and **F**). The inset in (**D**) shows a multi-shots acquisition where the discharge in the region right after the obstacle chooses different paths for different shots, before converging to a straight trajectory when self-healing takes place.

Figure 4

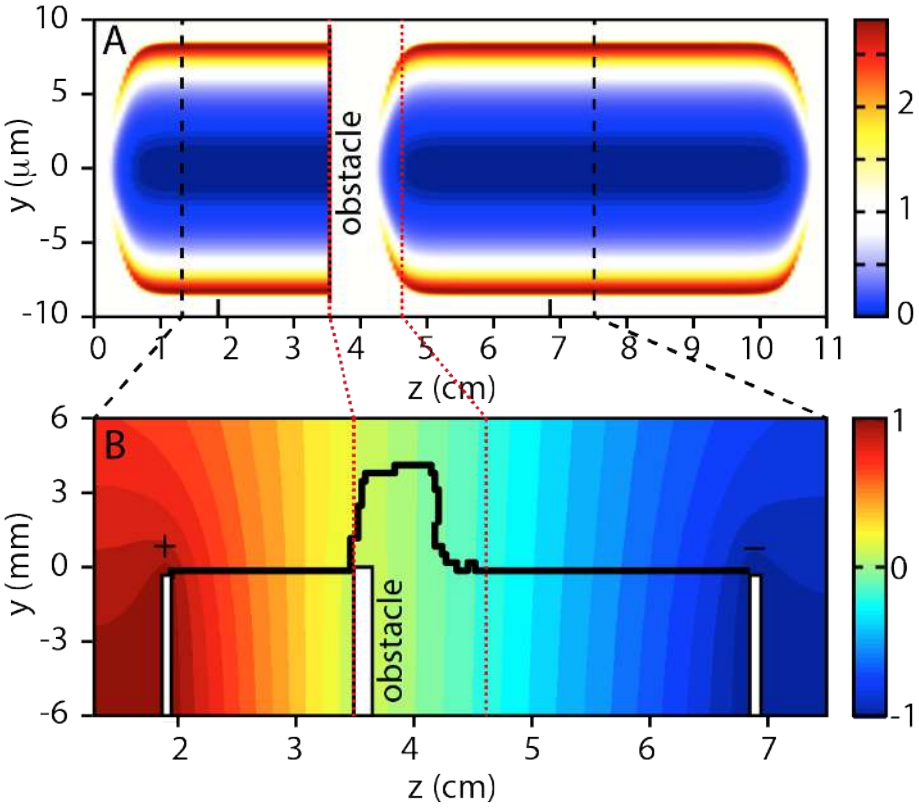

Figure 4. Air density profile. Simulation of the air density profile normalized to the ambient air density for the Bessel beam after 6.5 ns (**A**) and the corresponding discharge path (**B**). The colormap in (**B**) represents the initial normalized electric potential. Note that (**B**) shows a rescaled section of (**A**).

References and Notes:

1. K. H. Ho and S. T. Newman, "State of the art electrical discharge machining (EDM)," Int. J. Mach. Tools Manuf. **43**, 1287–1300 (2003).

2. D. T. Pham, S. S. Dimov, S. Bigot, A. Ivanov, and K. Popov, "Micro-EDM—recent developments and research issues," J. Mater. Process. Technol. **149**, 50–57 (2004).

3. A. Calka and D. Wexler, "Mechanical milling assisted by electrical discharge," Nature **419**, 147–51 (2002).

4. J. D. Dale, M. D. Checkel, and P. R. Smy, "Application of high energy ignition systems to engines," Prog. Energy Combust. Sci. **23**, 379–398 (1997).

5. W. Kim, H. Do, M. G. Mungal, and M. A. Cappelli, "Plasma-discharge stabilization of jet diffusion flames," IEEE Trans. Plasma Sci. **34**, 2545–2551 (2006).

6. J. R. Roth, "Aerodynamic flow acceleration using paraelectric and peristaltic electrohydrodynamic effects of a one atmosphere uniform glow discharge plasma," Phys. Plasmas **10**, 2117 (2003).

7. R. Hackam and H. Aklyama, "Air pollution control by electrical discharges," IEEE Trans. Dielectr. Electr. Insul. **7**, 654–683 (2000).

8. S. L. Daniels, "“On the ionization of air for removal of noxious effluvia” (Air ionization of indoor environments for control of volatile and particulate contaminants with nonthermal plasmas generated by dielectric-barrier discharge)," IEEE Trans. Plasma Sci. **30**, 1471–1481 (2002).

9. D. W. Koopman, "Channeling of an ionizing electrical streamer by a laser beam," J. Appl. Phys. **42**, 1883–1886 (1971).

10. M. Miki, Y. Aihara, and T. Shindo, "Development of long gap discharges guided by a pulsed CO 2 laser," J. Phys. D. Appl. Phys. **26**, 1244–1252 (1993).

11. X. M. Zhao and J. C. Diels, "Femtosecond pulses to divert lightning," Laser Focus World **29**, 113 (1993).

12. J.-C. Diels, R. Bernstein, K. E. Stahlkopf, and X. M. Zhao, "Lightning control with lasers," Sci. Am. **277**, 50–55 (1997).

13. M. Rodriguez, R. Sauerbrey, H. Wille, L. Wöste, T. Fujii, Y.-B. André, A. Mysyrowicz, L. Klingbeil, K. Rethmeier, W. Kalkner, J. Kasparian, E. Salmon, J. Yu, and J.-P. Wolf, "Triggering and guiding megavolt discharges by use of laser-induced ionized filaments," Opt. Lett. **27**, 772–774 (2002).

14. B. Forestier, A. Houard, I. Revel, M. Durand, Y. B. André, B. Prade, A. Jarnac, J. Carbonnel, M. Le Nevé, J. C. de Miscault, B. Esmiller, D. Chapuis, and A. Mysyrowicz, "Triggering, guiding and deviation of long air spark discharges with femtosecond laser filament," AIP Adv. **2**, 012151 (2012).

15. M. Scheller, N. Born, W. Cheng, and P. Polynkin, "Channeling the electrical breakdown of air by optically heated plasma filaments," Optica **1**, 125–128 (2014).

16. G. Siviloglou, J. Broky, A. Dogariu, and D. Christodoulides, "Observation of accelerating Airy beams," Phys. Rev. Lett. **99**, 213901 (2007).

17. J. Durnin, J. Miceli, and J. H. Eberly, "Diffraction-free beams," Phys. Rev. Lett. **58**, 1499–1501 (1987).

18. A. Couairon and A. Mysyrowicz, "Femtosecond filamentation in transparent media," Phys. Rep. **441**, 47–189 (2007).

19. F. Vidal, D. Comtois, A. Desparois, B. La Fontaine, T. W. Johnston, J.-C. Kieffer, H. P. Mercure, H. Pepin, and F. A. Rizk, "Modeling the triggering of streamers in air by ultrashort laser pulses," IEEE Trans. Plasma Sci. **28**, 418–433 (2000).

20. S. Tzortzakis, B. Prade, M. Franco, A. Mysyrowicz, S. Hüller, and P. Mora, "Femtosecond laser-guided electric discharge in air," Phys. Rev. E **64**, 057401 (2001).

21. J. Meek, "A theory of spark discharge," Phys. Rev. **57**, 722–728 (1940).

22. D. G. Papazoglou, S. Suntsov, D. Abdollahpour, and S. Tzortzakis, "Tunable intense Airy beams and tailored femtosecond laser filaments," Phys. Rev. A **81**, 061807 (2010).

23. P. Polynkin, M. Kolesik, J. V Moloney, G. A. Siviloglou, and D. N. Christodoulides, "Curved plasma channel generation using ultraintense Airy beams," Science (80-.). **324**, 229–232 (2009).

24. A. Minovich, A. E. Klein, N. Janunts, T. Pertsch, D. N. Neshev, and Y. S. Kivshar, "Generation and near-field imaging of Airy surface plasmons," Phys. Rev. Lett. **107**, 116802 (2011).

25. C. J. Zapata-Rodríguez, S. Vuković, M. R. Belić, D. Pastor, and J. J. Miret, "Nondiffracting Bessel plasmons," Opt. Express **19**, 19572–19581 (2011).

26. I. Kaminer, R. Bekenstein, J. Nemirovsky, and M. Segev, "Nondiffracting accelerating wave packets of Maxwell's equations," Phys. Rev. Lett. **108**, 163901 (2012).

27. F. Courvoisier, A. Mathis, L. Froehly, R. Giust, L. Furfaro, P. A. Lacourt, M. Jacquot, and J. M. Dudley, "Sending femtosecond pulses in circles: highly nonparaxial accelerating beams," Opt. Lett. **37**, 1736–1738 (2012).

28. P. Zhang, Y. Hu, D. Cannan, A. Salandrino, T. Li, R. Morandotti, X. Zhang, and Z. Chen, "Generation of linear and nonlinear nonparaxial accelerating beams," Opt. Lett. **37**, 2820–2822 (2012).

29. P. Zhang, Y. Hu, T. Li, D. Cannan, X. Yin, R. Morandotti, Z. Chen, and X. Zhang, "Nonparaxial Mathieu and Weber accelerating beams," Phys. Rev. Lett. **109**, 193901 (2012).

30. I. Chremmos and N. Efremidis, "Nonparaxial accelerating Bessel-like beams," Phys. Rev. A **88**, 063816 (2013).

31. R. P. MacDonald, S. A. Boothroyd, T. Okamoto, J. Chrostowski, and B. A. Syrett, "Interboard optical data distribution by Bessel beam shadowing," Opt. Commun. **122**, 169–177 (1996).

32. Z. Bouchal, J. Wagner, and M. Chlup, "Self-reconstruction of a distorted nondiffracting beam," Opt. Commun. **151**, 207–211 (1998).

33. J. Broky, G. a Siviloglou, A. Dogariu, and D. N. Christodoulides, "Self-healing properties of optical Airy beams," Opt. Express **16**, 12880–12891 (2008).

34. A. Couairon, E. Brambilla, T. Corti, D. Majus, O. de J. Ramírez-Góngora, and M. Kolesik, "Practitioner's guide to laser pulse propagation models and simulation," Eur. Phys. J. Spec. Top. **199**, 5–76 (2011).

35. E. F. Toro, *Riemann Solvers and Numerical Methods for Fluid Dynamics* (Springer, 2009).

36. Y.-H. Cheng, J. K. Wahlstrand, N. Jhajj, and H. M. Milchberg, "The effect of long timescale gas dynamics on femtosecond filamentation," Opt. Express **21**, 4740–4751 (2013).

37. L. Niemeyer, L. Pietronero, and H. J. Wiesmann, "Fractal dimension of dielectric breakdown," Phys. Rev. Lett. **52**, (1984).

38. X. Yang, J. Wu, Y. Peng, Y. Tong, P. Lu, L. Ding, Z. Xu, and H. Zeng, "Plasma waveguide array induced by filament interaction," Opt. Lett. **34**, 3806–8 (2009).

39. H. Cai, J. Wu, H. Li, X. Bai, and H. Zeng, "Elongation of femtosecond filament by molecular alignment in air," Opt. Express **17**, 21060–21065 (2009).

40. X. M. Zhao, J. -C. Diels, C. Y. Wang and J. M. Elizondo, "Femtosecond Ultraviolet Laser Pulse Induced Lightning Discharges in Gases," IEEE J. Quantum Electron. **31**, 599 (1995).

41. G. Point, C. Milián, A. Couairon, A. Mysyrowicz, and A. Houard, "Generation of Long-lived Underdense Channels using Femtosecond Filamentation in air," J. Phys. B: At. Mol. Opt. Phys. **48,** 094009 (2015).

42. I. Dolev, I. Kaminer, A. Shapira, M. Segev, and A. Arie, "Experimental Observation of Self-Accelerating Beams in Quadratic Nonlinear Media," Phys. Rev. Lett. **108**, 113903 (2012).

Acknowledgments:

RM and FL gratefully acknowledge MERST, NSERC, FQRNT for funding this work. MC acknowledges the support from the People Program (Marie Curie Actions) of the European Union's Seventh Framework Program (FP7/2007-2013) under REA grant agreement No. (299522). The work of DNC was supported by the Air Force Office of Scientific Research (MURI Grant No. FA9550-10-1-0561), and ZC by the AFOSR and NSF. The experiments have been carried out at the ALLS facility located at the INRS-EMT. Competing Interests: The authors declare that they have no competing interests.

Supplementary Materials:

Supplementary Text

Figures S1-S3

References (*41-42*)